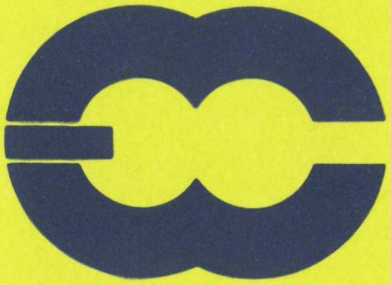

European Centre
for Medium Range
Weather Forecasts

Verification and Storing with Empirical Orthogonal Functions

Internal Report No 18
Research Dept.

November 1978

Centre Européen pour les Prévisions Météorologiques
à Moyen Terme

Europäisches Zentrum für mittelfristige Wettervorhersage

VERIFICATION AND STORING WITH EMPIRICAL ORTHOGONAL FUNCTIONS

By

Hannu Savijärvi

European Centre for Medium Range Weather Forecasts
Bracknell, U.K.

Internal Report No. 18

Research Department

A B S T R A C T

Empirical orthogonal functions (e.o.f.) for 500 mb height field from 20 years' material (Karhila and Rinne, 1977) have been used in expanding analyses from different weather services as well as ECMWF forecasts into e.o.f. series $z(x,y,t) = \overline{z(x,y)} + \sum_{n=1}^{175} c_n(t)\, f_n(x,y)$. The largest (still small) deviation between simultaneous NMC, DWD and FNWC[1)] analyses occurs in c_2. The deviation between 10-day forecast and NMC analysis is by far the largest in c_1, indicating problems in model physics, as c_1 has a profound yearly cycle. Use of persistence for c_1 in rebuilding the forecast gives 10% better rms error score. An attempt has also been made to explore the efficiency in using e.o.f.'s to store meteorological fields. For the same amount of numbers to be stored (these) e.o.f.'s are about twice as effective as spherical harmonics expansion, measured by the maximum deviation and rms deviation of 500 mb height field in NMC grid, but may filter out rare events.

1) NMC - National Meteorological Center, U.S.A.
DWD - Deutscher Wetterdienst, Federal Republic of Germany
FNWC - U.S. Navy Fleet Numerical Weather Central, U.S.A.

1. Introduction

Following the Workshop on the use of empirical orthogonal functions in meteorology (ECMWF,1977) some work has been done in ECMWF on the verification and storing of forecasts with the aid of horizontal empirical orthogonal functions (e.o.f.'s) of the 500 mb height field. These functions have been calculated in the Department of Meteorology, University of Helsinki, on a very large material. They are described briefly in Section 2. The comparison of three numerical analyses with the aid of e.o.f.'s is in Section 3, verification, statistical correction and smoothing tests are in Sections 4 and 5, and finally a straightforward comparison in storing effectivity is made between e.o.f.'s and spherical harmonic expansion in Section 5.

2. Horizontal empirical orthogonal functions

There are different approaches in defining the empirical orthogonal functions (e.g. Holmström, 1977). Computations are, however, usually based on finding them as eigenvectors f_n related to eigenvalues λ_n of the covariance matrix M:

$$Mf_n = \lambda_n f_n \tag{2.1}$$

where the elements M_{ij} of M are

$$M_{ij} = \frac{1}{T} \sum_{t=1}^{T} [z(i,t) - zm(i)] \; [z(j,t) - zm(j)] \tag{2.2}$$

for the atmospheric variable z(x,y,t) given in discrete points i,t, (N in space and T in time) with the time mean

$$zm(i) = \frac{1}{T} \sum_{t=1}^{T} z(i,t) \tag{2.3}$$

The eigenvectors (e.o.f.'s, principal components) $f_n(i)$ are classified according to decreasing magnitude of eigenvalues, the sum of which gives the total variance in the data sample:

$$\sigma^2 = \frac{1}{T}\sum_{t=1}^{T}\{\frac{1}{N}\sum_{i=1}^{N}[z(i,t)-zm(i)]^2\} = \sum_{n=1}^{N}\lambda_n \qquad (2.4)$$

The eigenvectors are orthogonal and usually normalised to one over the definition area A :

$$\frac{1}{A}\int_A f_n\, f_m\, da \cong \sum_{i=1}^{N} f_n(i)f_m(i)da(i)=\delta_{nm}; \sum_{i=1}^{N} da(i) = 1 \qquad (2.5)$$

Here da(i) is the dimensionless area element for the grid point i.
Once the functions have been determined the variable z(i,t) can be presented in the series expansion

$$z(i,t) = zm(i) + \sum_{n=1}^{N} c_n(t)\, f_n(i) \qquad (2.6)$$

Multiplying (2.6) by $f_n(i)$, integrating over the area A and using the orthonormality condition (2.5) gives the coefficients c_n:

$$c_n(t) = \sum_{i=1}^{N}(z(i,t) - zm(i))f_n(i)da(i) \qquad (2.7)$$

The series (2.6) is exact (without any residual) if all possible N components are used. Because e.o.f.'s are by definition the most rapidly converging series expansion in the data sample (in r.m.s. sense) , the components related to small eigenvalues can be left out without introducing too much residual in the series (2.6). This property makes e.o.f. expansion possibly useful for storing and smoothing purposes.

ECMWF has received the functions determined in the e.o.f. project of the Department of Meteorology, University of Helsinki. The data material is from the U.S. Navy Fleet Numerical Weather Central (FNWC), Monterey, California, altogether T = 11876 500 mb height analyses from 20 years between 1945 and 1970. The area for computations is the NMC grid north from 22° N in N = 1404 grid points. This very large material was divided into four coarser grids, e.o.f.'s were determined for each coarse grid and finally joined together. The detailed method and data description is in Karhila and Rinne (1977), the accuracy of the series is discussed in Rinne and Järvenoja (1977) and data checking with the resulting e.o.f.'s is indicated in Rinne (1977).

Figure 1 shows the first six e.o.f.'s with their contribution to the total variance of the data $\sim(159\ \mathrm{m})^2$. The first function f_1 has large values over the eastern part of the continents (the climatological trough areas) and lower values over oceans. The time series of the first coefficient c_1 has a clear yearly cycle being negative in winter and positive in summer. Thus the combination $c_1 f_1$ tends to strengthen the main troughs in winter and weaken them in summer, a feature typical for all e.o.f. investigations where the yearly cycle is not excluded (c.f. Craddock and Flood, 1969).

The other coefficients do not have any clear cycles. The patterns of the higher functions depend fully on the data sample and thus not too much weight should be given to individual e.o.f.'s or their physical meaning.

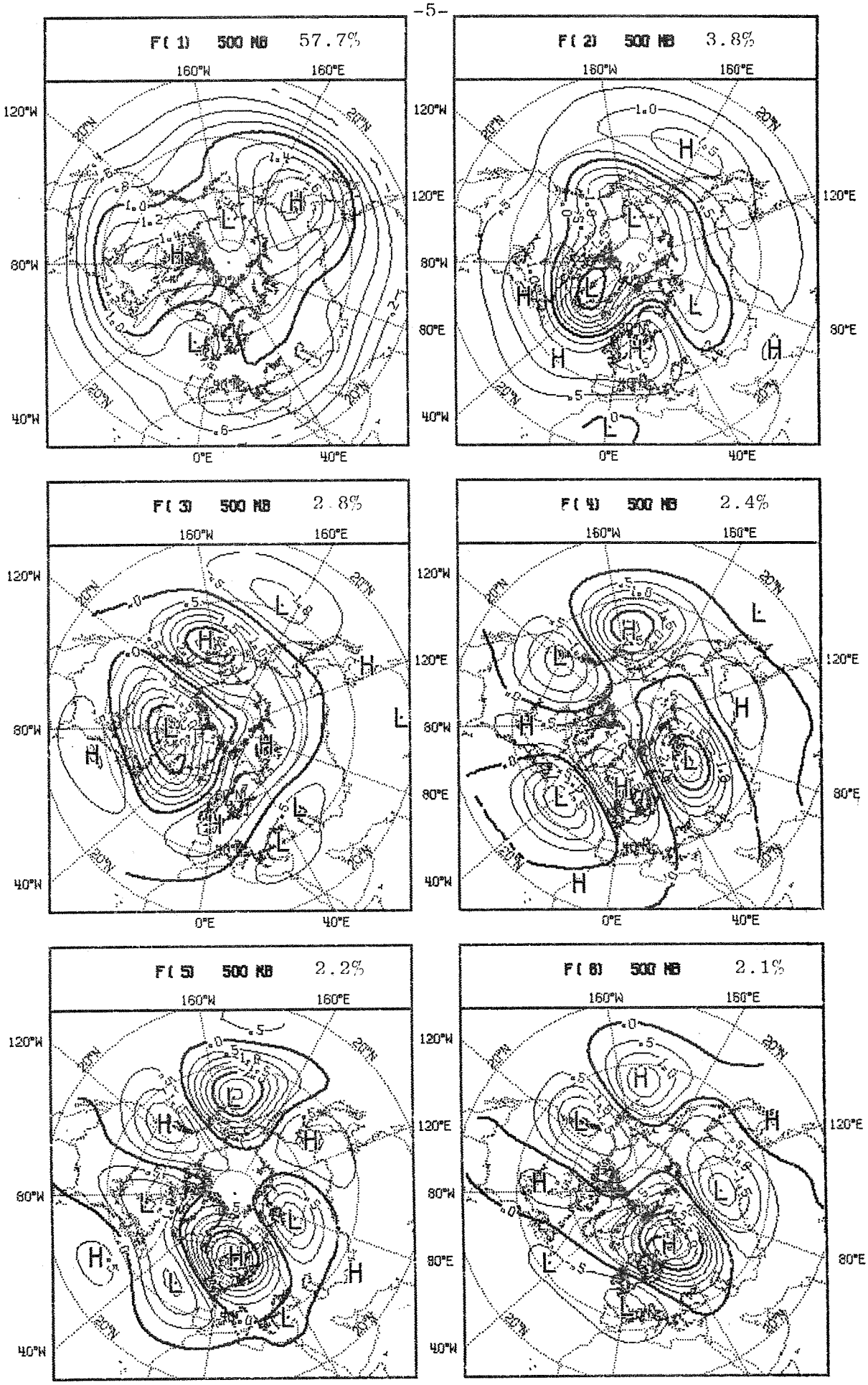

Fig. 1 The six first e.o.f.'s and their variance reduction

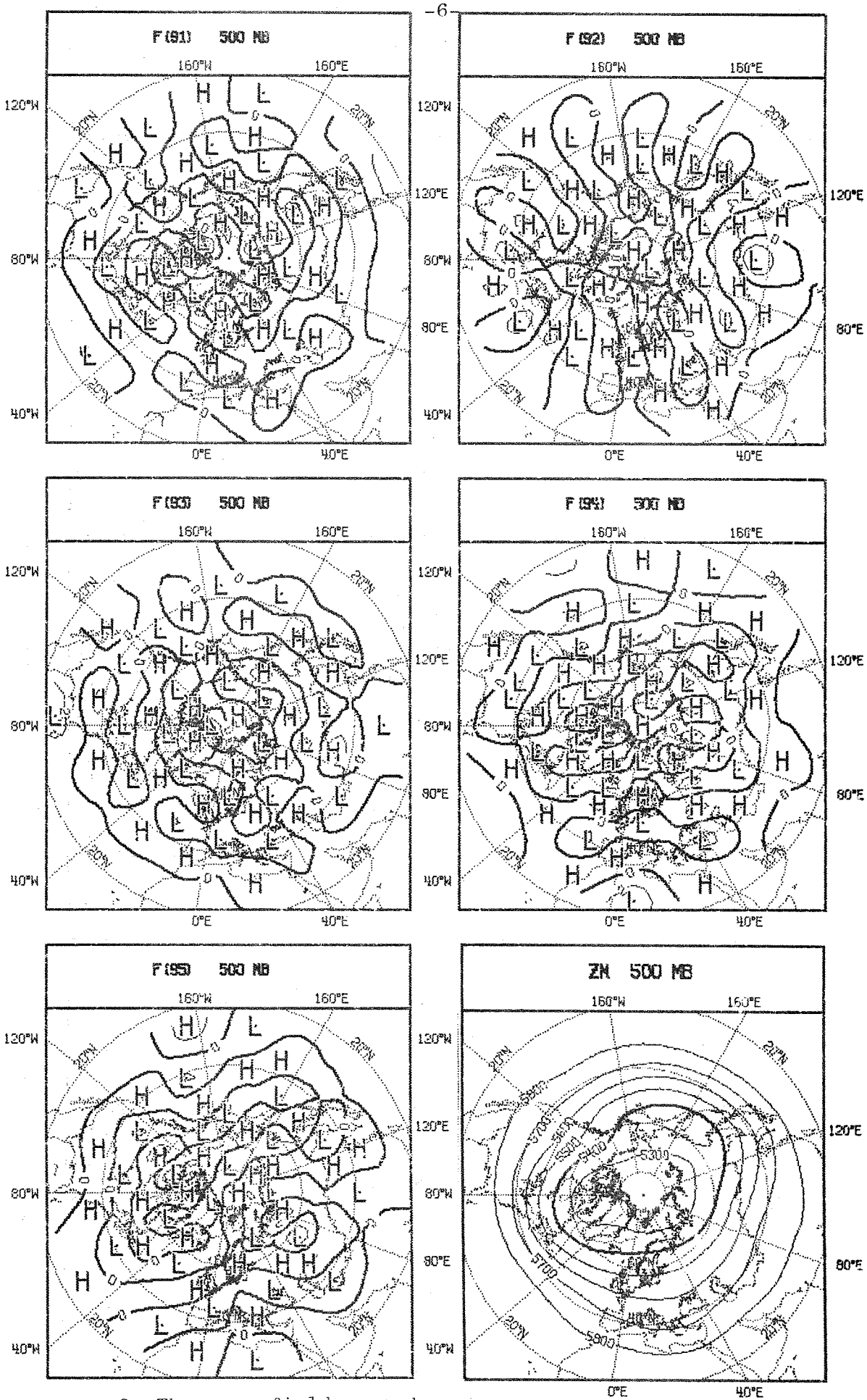

Fig. 2. The mean field zm and e.o.f.'s 91 - 95.

Figure 2 shows the 20 year mean field zm and the functions 91 - 95 as examples of the smaller spatial scales involved with the higher functions. In all, 175 functions will be used in the following. Their cumulative variance reduction is 99.50 % in the 20 year data sample.

3. Comparison of three numerical analyses

Otto-Bliesner et al (1977) found differences in simultaneous numerical analyses of 500 mb height fields in a data-rich U.S. continental area. Comparison of NMC and DWD analyses from December 1970 to January 1971 in ECMWF (Arpe, 1977, unpublished report) revealed considerable and systematic differences between the two analyses, NMC having generally stronger gradients and more kinetic energy in geostrophic wind in all zonal wave numbers, especially in the subtropics. To find out the normal scale of deviations in the time series of e.o.f. coefficients three analyses available in ECMWF for December 1970 were compared. Two of them were made with the correction method, NMC using forecast as a first guess, DWD starting from climatology. FNWC analyses were made by a modified correction method (see Haltiner, 1971). They are dependent data, being included in the 20 year data sample used in the determination of the e.o.f.'s . The DWD analyses were interpolated to the NMC grid and e.o.f. coefficients $c_n(t)$ were computed for all the three analyses using equation (2.7).

Figures 3, 4 and 5 show the time series of some e.o.f. coefficients for 16 days of December 1970. In general, the daily change in the first coefficients is smooth. For the first coefficient c_1, NMC gives smaller absolute values than DWD and FNWC, while in the second coefficient the difference between the three analyses is quite large. In higher modes the analyses seem to agree better, DWD possibly giving slightly smoother time series. The two American analyses with supposedly rather similar observational data background seem to agree well in higher modes, which describe smaller scale phenomena. The normal initial variance in the coefficients is, according to this data, well within 10 m, except for the first two coefficients. The ability of the functions in describing independent material (DWD and NMC) seems to be rather good.
The mean rms difference between NMC and DWD analyses $\text{rmsd} = \sqrt{(z_{NMC} - z_{DWD})^2}^{\text{area}}$ was 30.5 m north from 22°N in December 1970. Using the orthogonality of the e.o.f. series (2.6) the mean square deviation can be written as the sum of contributions from each mode and thus rmsd is :

$$\text{rmsd} = \sqrt{\sum_{n=1}^{N} (C_n^{NMC}(t) - C_n^{DWD}(t))^2} \qquad (3.1)$$

In Figure 6 the rms difference(3.1) is plotted as the function of the cumulative sum index, for 30 day mean as well as for one individual case. Most of the difference comes from the lower modes; one third of the monthly mean rms deviation is obtained with the modes 1 - 10 and one half is obtained with the first 20 modes. Consequently the differences between the analyses are not only small scale features.

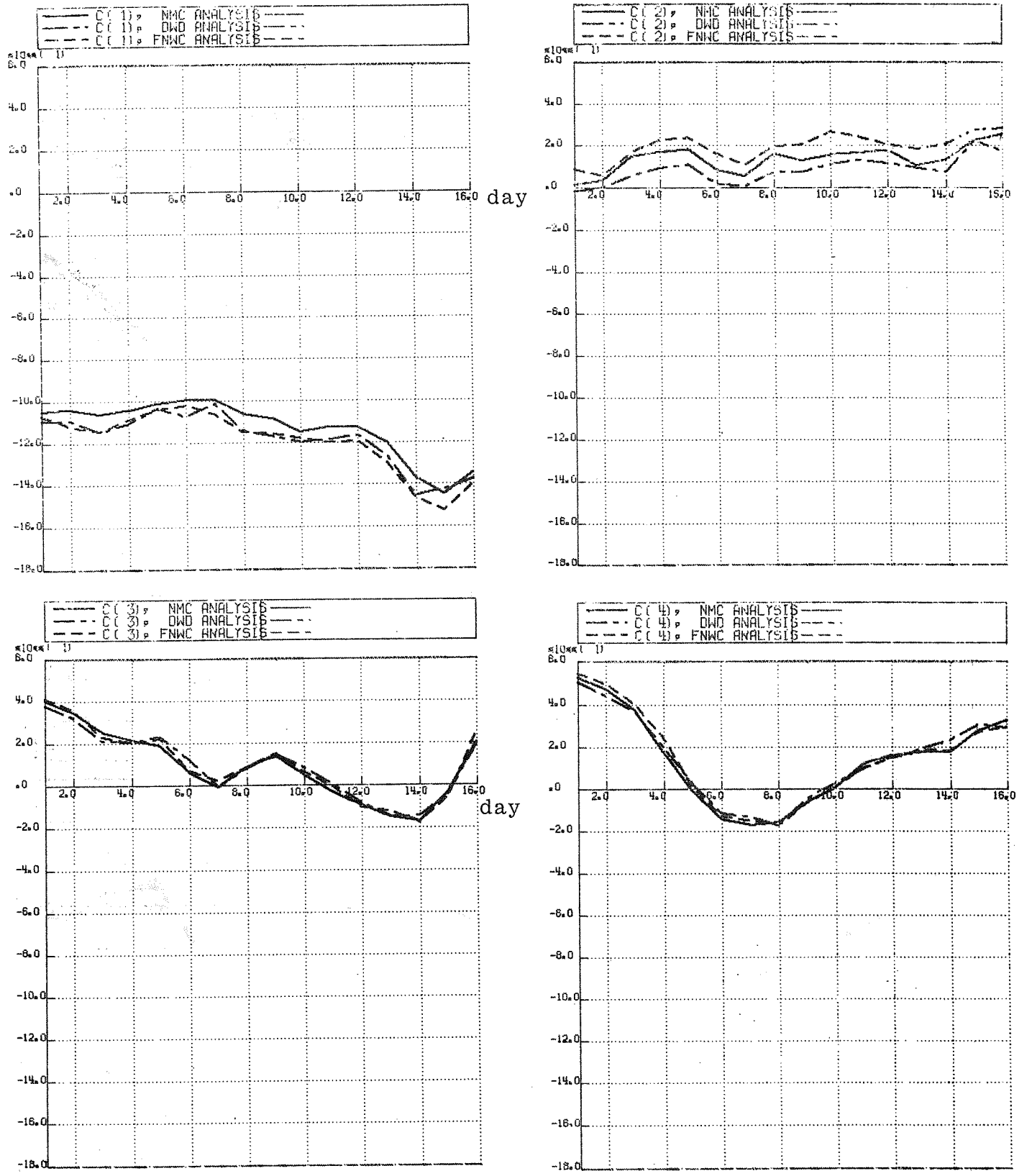

Fig. 3 . c_1-c_4 for 3 objective analyses in December 1-16 1970.
Unit: 10 m.

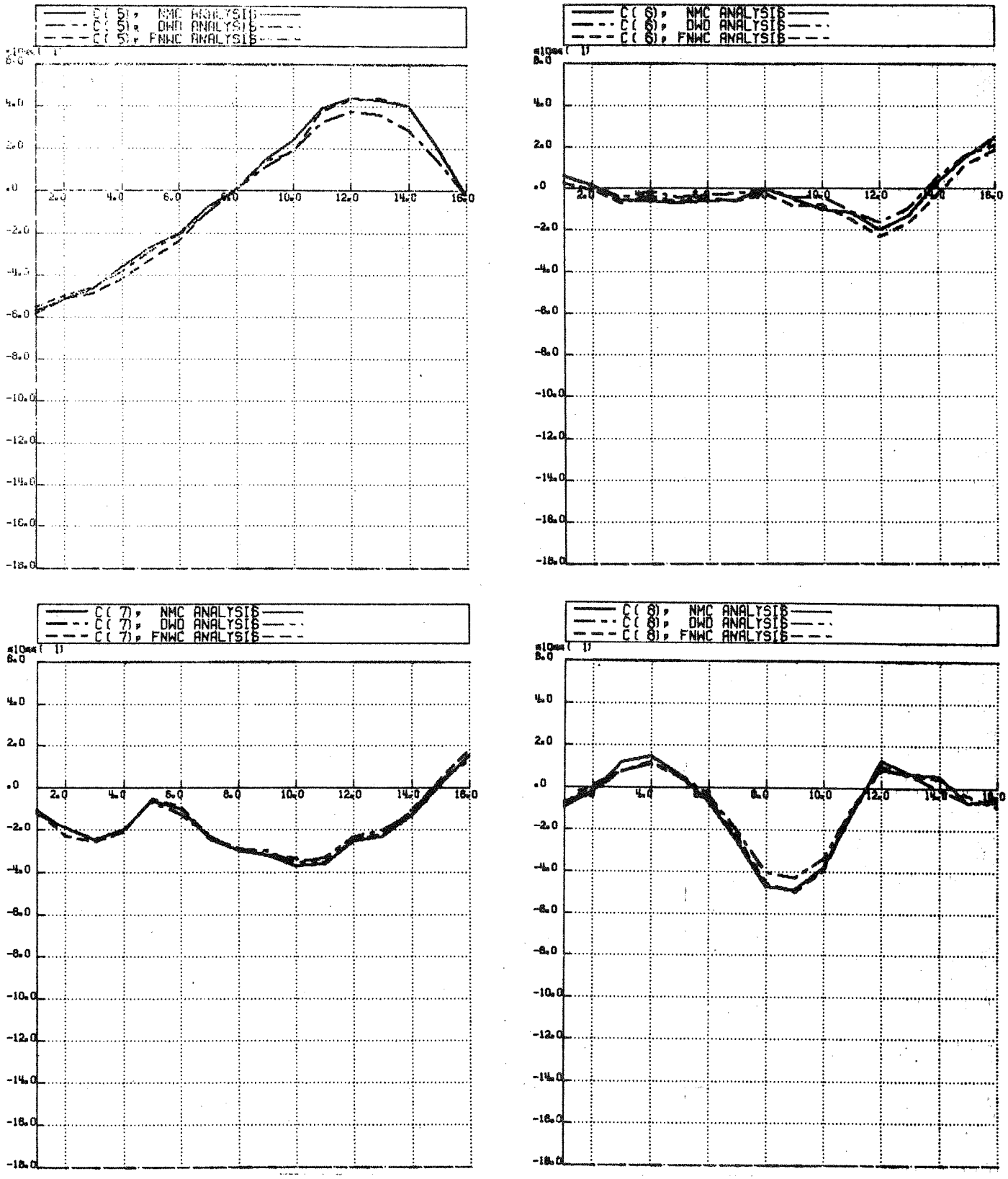

Fig. 4. c_5-c_8 for 3 analyses. December 1-16 1970.

Unit: 10 m.

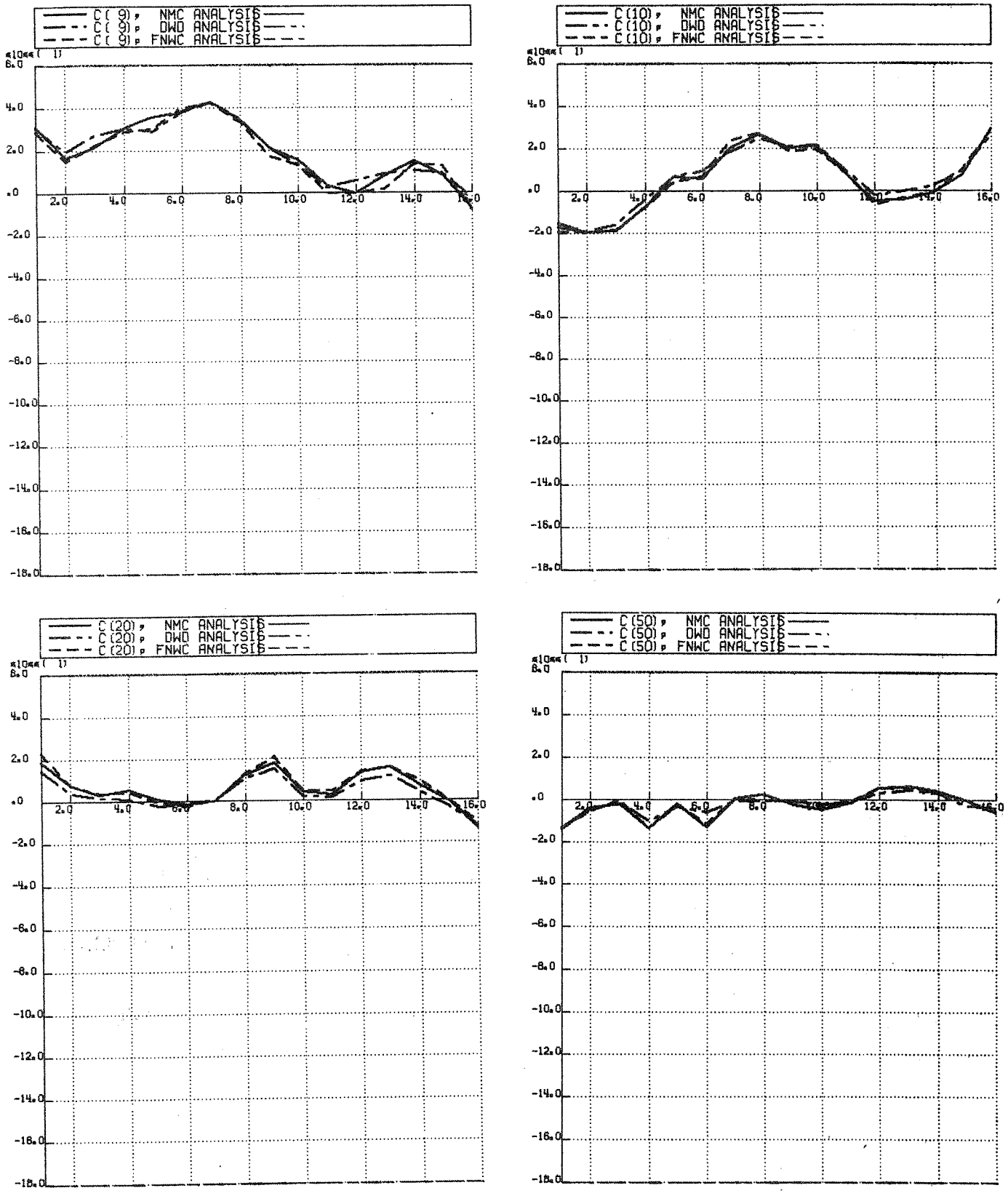

Fig. 5. $c_9, c_{10}, c_{20}, c_{50}$ for 3 analyses. December 1-16 1970.

Unit: 10 m.

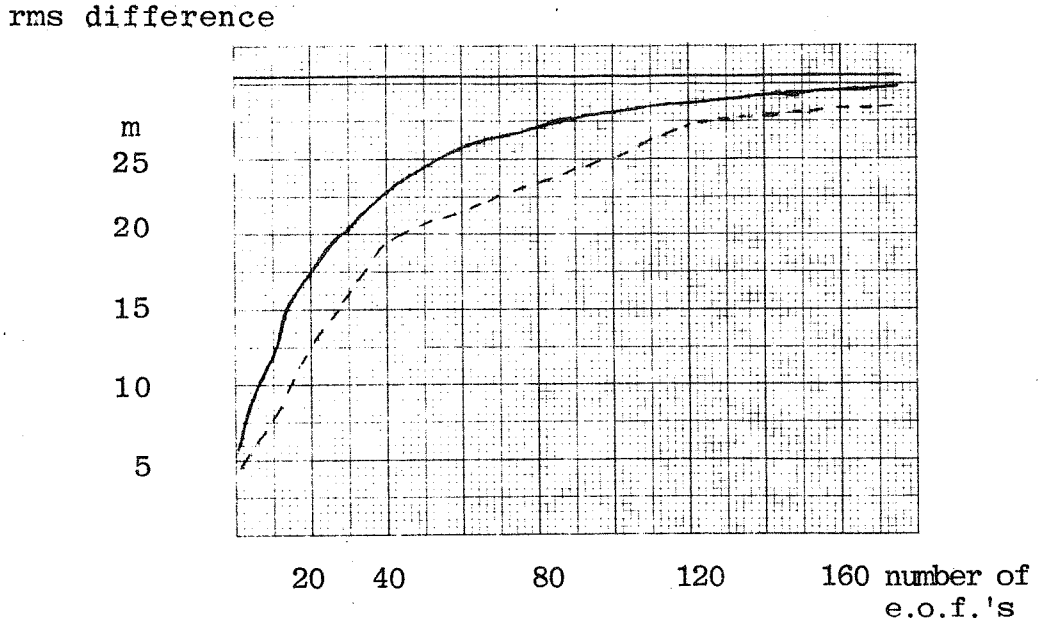

Fig. 6. Rms difference between NMC and DWD in 500 mb height analyses, December 1970.
——— 30 day mean ---- 1.12.1970 0z

4. Verification trials

The 10 day forecast used in the verification test was made by the ECMWF N16/24 9 level model*) with GFDL physics but Kuo-type moist convection scheme, starting from the GFDL initial data set for 1.3.1965 00 GMT. This version of the model and the quality of the forecast was discussed as experiment N02 in Tiedtke (1977). The 500 mb height fields were interpolated to the e.o.f. grid and coefficients $c(t)$ computed from (2.7). NMC analyses are used for verification.

Figure 7 presents the first coefficients in the 10 day interval for the forecast and verification fields. The initial difference between the GFDL and NMC analyses is small except for the first coefficient. This initial difference in c_1 indicated a small error in the pre-processing of initial data, which was found and cured later.

*) N16/24: 16 points in 90° longitude, $\Delta\lambda = 5.625^\circ$
24 points in 90° latitude, $\Delta\phi = 3.75^\circ$

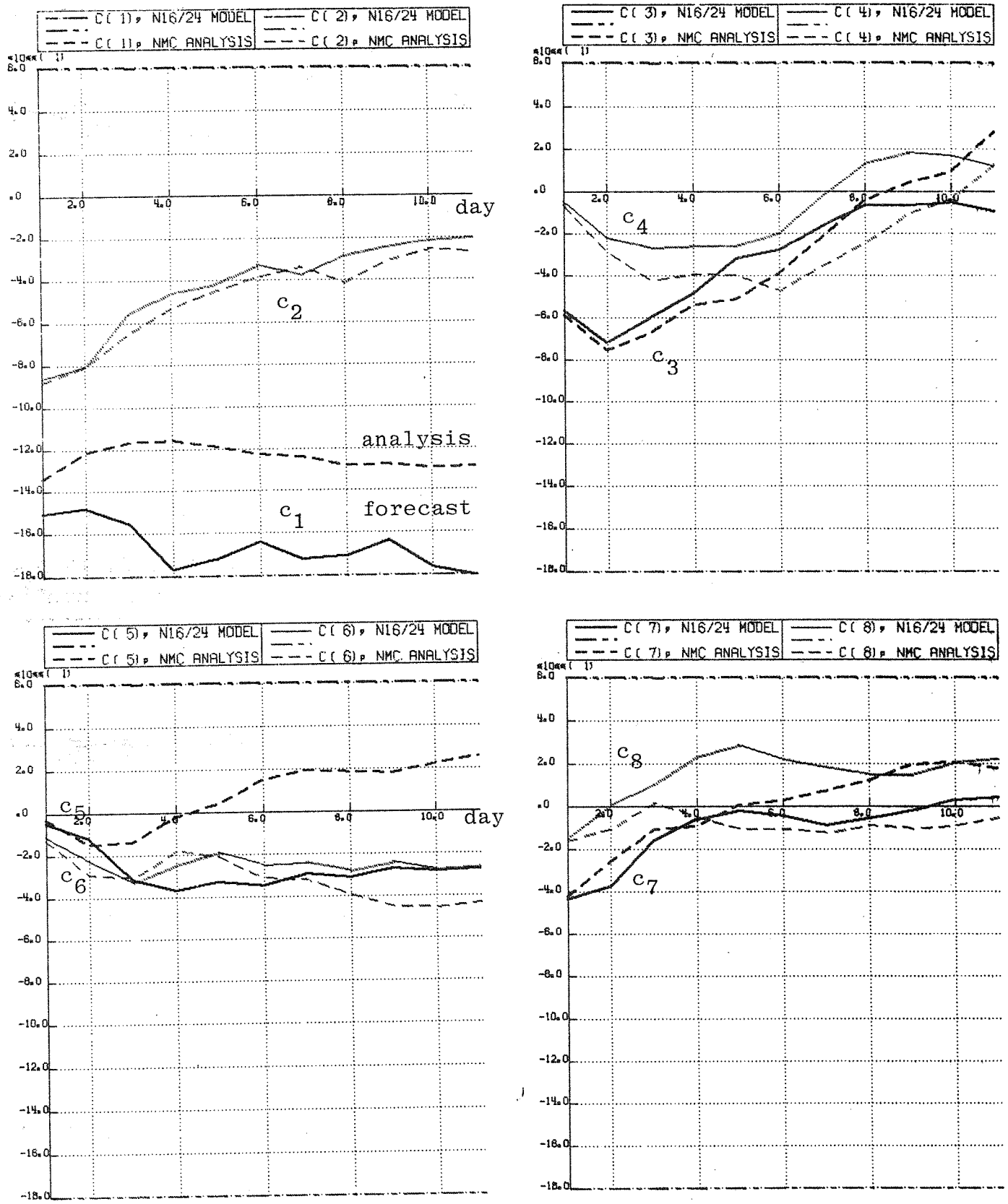

Fig. 7. $c_1 - c_8$ for NMC analyses and 10 day forecast with ECMWF N16/24 model. March 1-11 1965. Unit: 10 m.

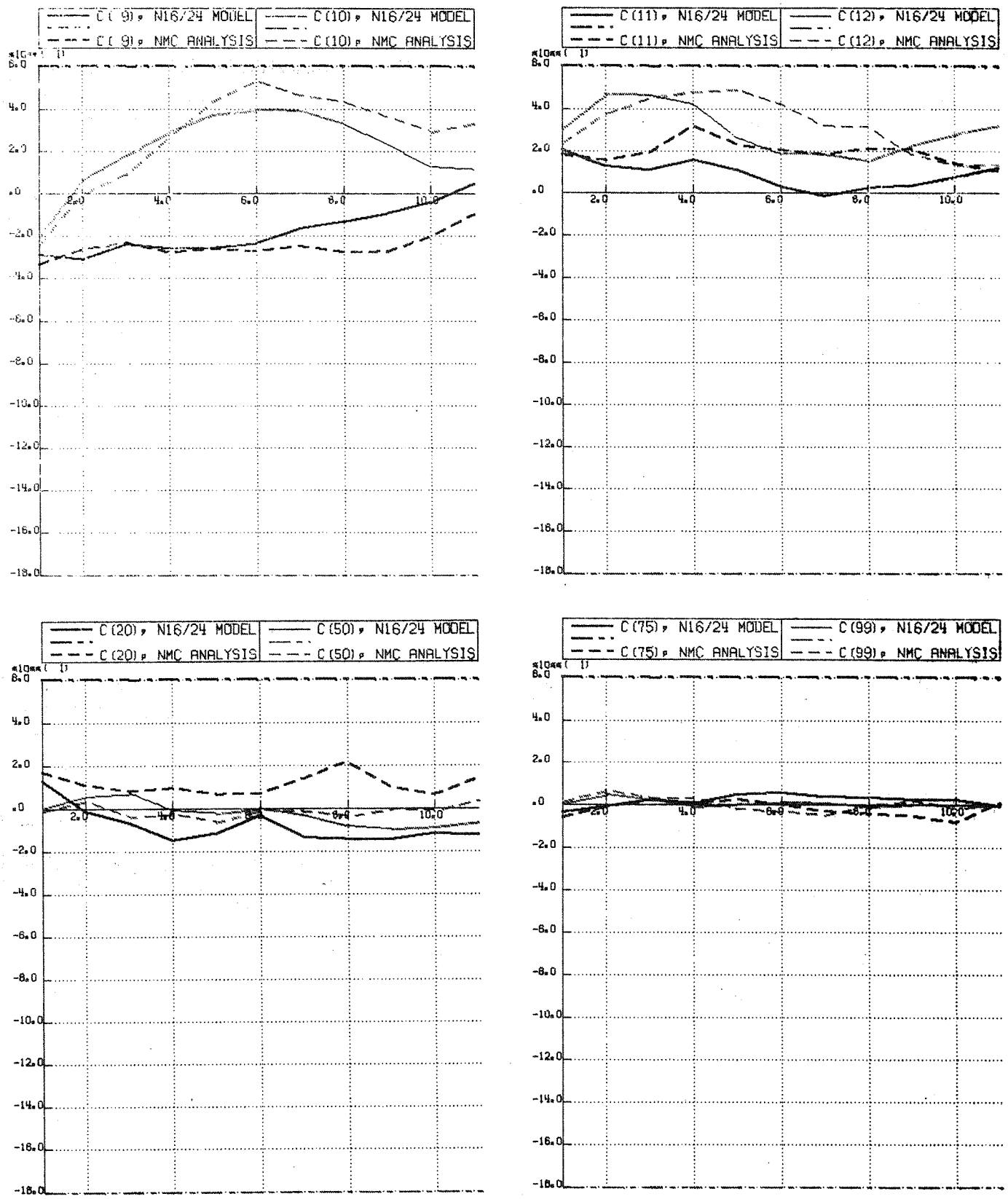

Fig. 8. As Fig. 7 but for c_9 - c_{12}, c_{20}, c_{50}, c_{75}, c_{99}

The forecast error, measured as the difference between analyses c_n and forecast c_n, is by far largest in the first coefficient, being 40 - 50 m after 3 days.

The first e.o.f. component is related to climate through the annual cycle of the first coefficient and the land-sea distribution of the pattern itself. The large error in the first coefficient may thus indicate problems in the climatologically important features of the model, which are topography and heat sources and sinks, i.e. what we usually denote 'physics'. In the second coefficient the deviation between the forecast and analysis remains smaller than between two analyses, while the third and fourth modes show a slow but successive deviation from the analyses through the forecast period. The error is again large for coefficient 5, where even the sign is wrong. The most dominant feature in function 5 was the high - low pair over the Atlantic-Pacific oceans. This negative correlation pattern is very similar to the surface pressure anomaly maps in cold/warm northern winters in van Loon and Rogers (1977).

Expansion of rms-error and correlation coefficient of anomalies from the time-mean zm with e.o.f. series gives

$$\text{rmse}(n1,n2) = \sqrt{\sum_{n=n1}^{n2} (C_n^o(t) - C_n^f(t))^2} \qquad \text{o=observed} \tag{4.1}$$

$$\text{corr}(n1,n2) = \frac{\sum_{n=n1}^{n2} C_n^o(t)\, C_n^f(t)}{\sqrt{\sum_{n=n1}^{n2} C_n^o(t)^2 \sum_{n=n1}^{n2} C_n^f(t)^2}} \qquad \text{f=forecast} \tag{4.2}$$

Figure 9 shows these error scores for the 10 day forecast together with persistence and climatological normal rms variation. In the verification area north of 22°N the grid point scores and (4.1) and (4.2) are practically the same, when all 175 components are included, so that very little contribution is coming from modes higher than

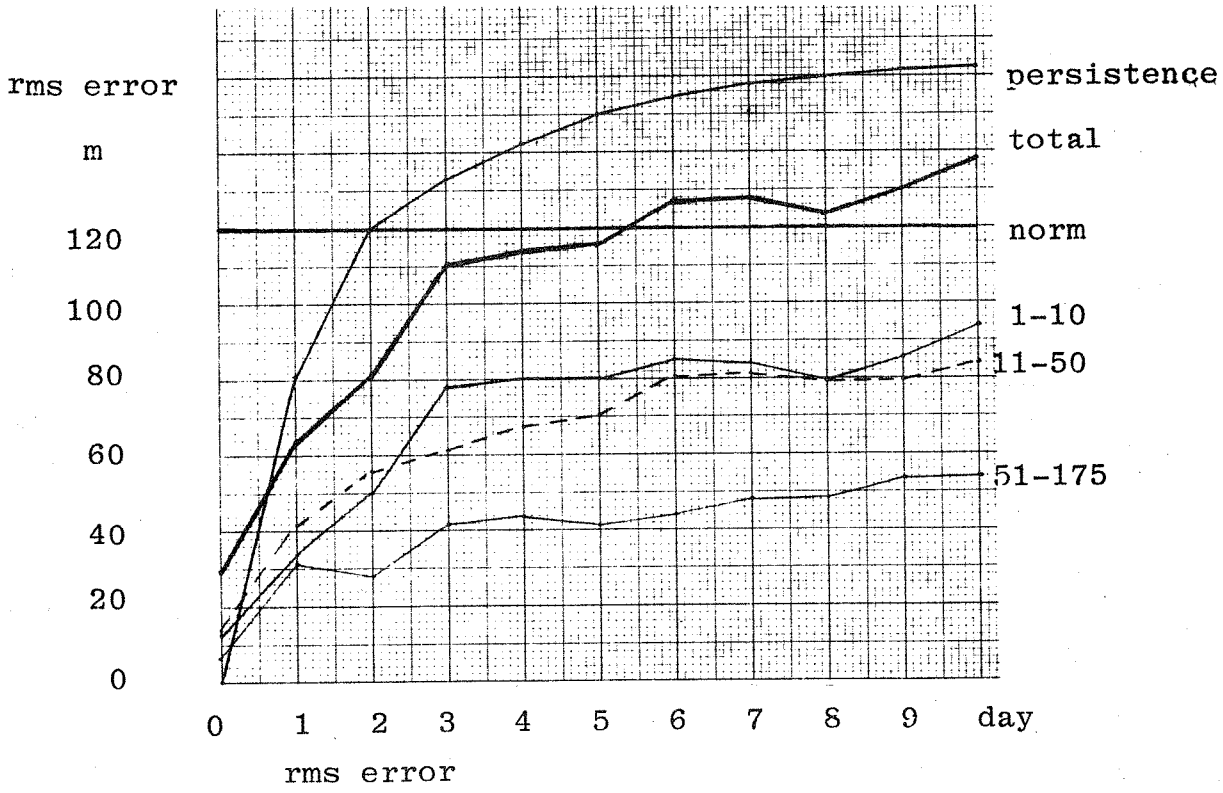

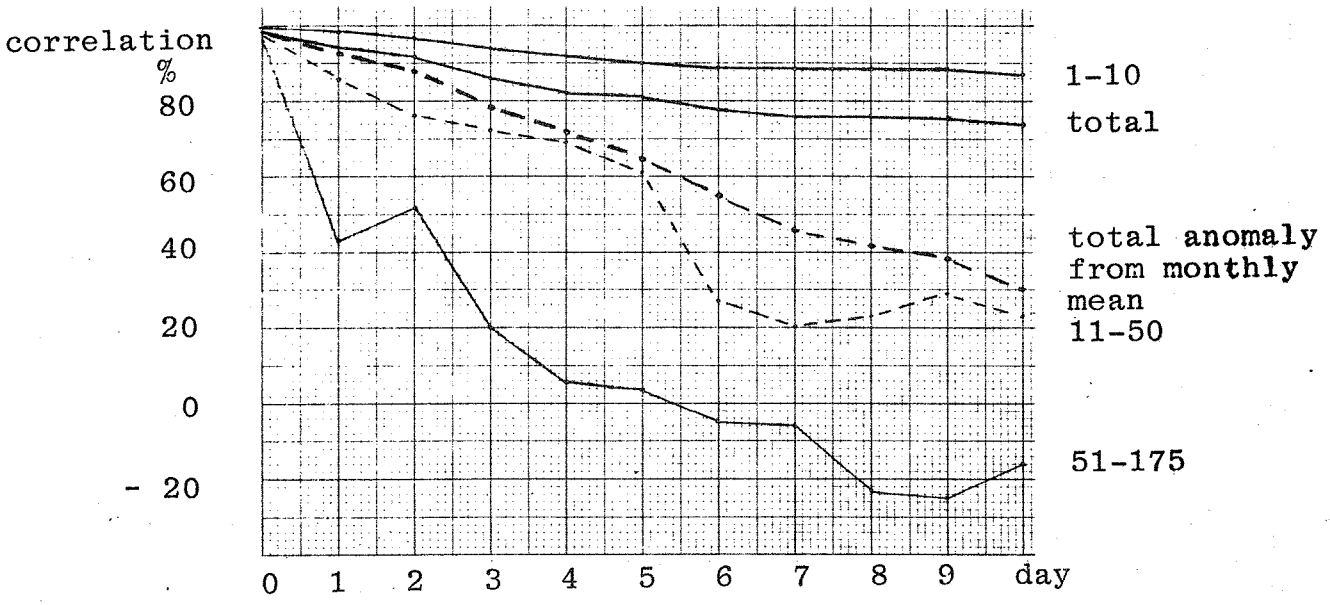

Fig. 9. 500 mb height verification scores expanded into e.o.f. series. ECMWF N16/24 model, 10 day forecast from 1.3.1965 0Z

175. Most of the difference is due to the lower modes 1 - 10 and 11 - 50, in about the same proportion. This was also the case for the differences between analyses (see also day 0 for NMC and GFDL analyses) and it is expected that the rms error curve rmse as the function of n would look much similar to Figure 6.

The high correlation coefficients in Figure 9 are partly due to the 20 year time mean zm used in the anomaly. Taking instead the climatological mean for March as in the ECMWF verification system changes the correlation curve considerably (thick dashed line in Fig. 9). Similar effect is obtained by using "daily" climate zm + $c_1(t)\ f_1$ instead of zm for the correlation coefficient expansion (4.2).

5. Dynamical-statistical forecasting

The smooth behaviour and large forecast error in the first coefficient suggest to keep it constant and equal to initial value when reconstructing the grid point values. This should decrease error in the resulting forecast field. This combination of persistence (for c_1) and forecast (for c_n, $n > 1$), was tried.

Figure 10 gives the rms error and Figure 11 the forecast z 500 field for day 5. In this case study the rms error decreased about 10 % and the reconstructed forecast pattern is more realistic e.g. in the low pressure systems over U.S. west coast.

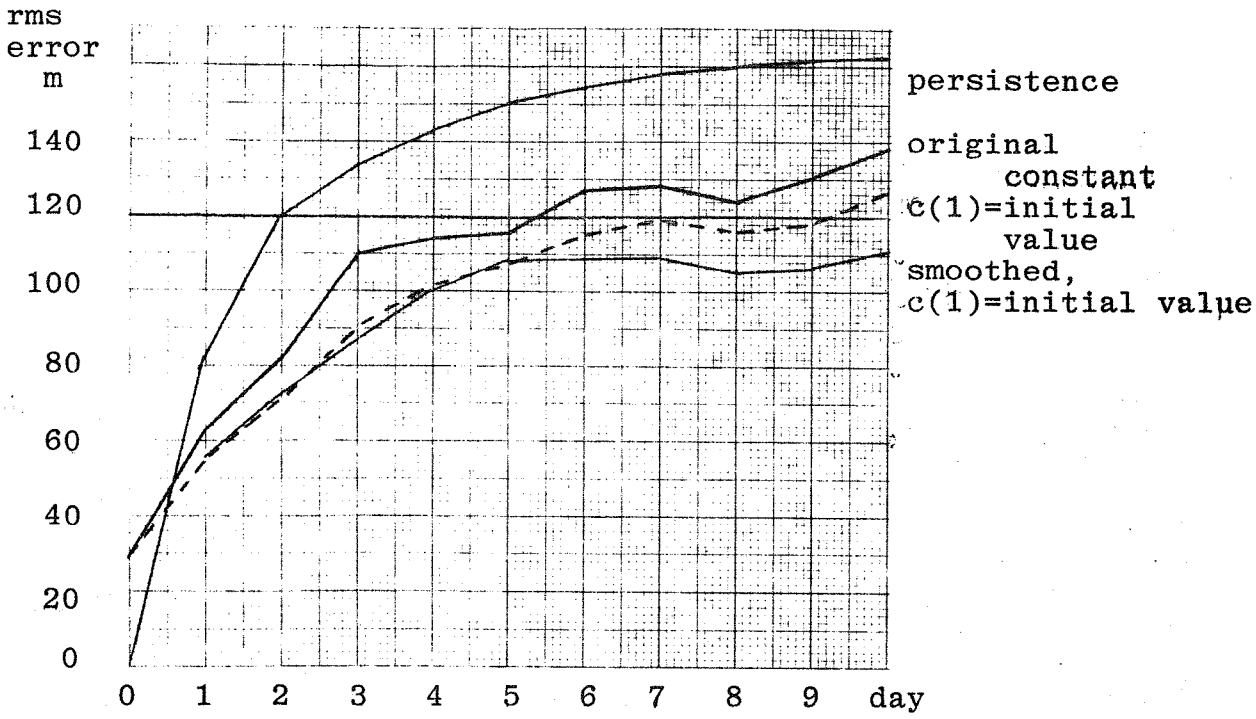

Fig. 10. Rms error for reconstructed forecast

In an attempt to reduce rms error of the forecast Rinne (1972) developed a regression model between e.o.f. coefficients in a sample of analyses and forecasts from a filtered three parameter model. The rms error minimizing regression equations appeared to be a smoothing scheme, according to which each $c_n(t)$ of the forecast should be multiplied by B(n,t),

$$B(n,t) = e^{-0.22(T-1) - 0.009\,n} \qquad (5.1)$$

where T is the forecast period in days. This smoothing was quite strong and a weaker smoother was applied in a barotropic model based on e.o.f.'s (Rinne & Karhila,1975), where

$$B(n,t) = e^{-0.11(T-0.5) - 0.009\,n} \qquad (5.2).$$

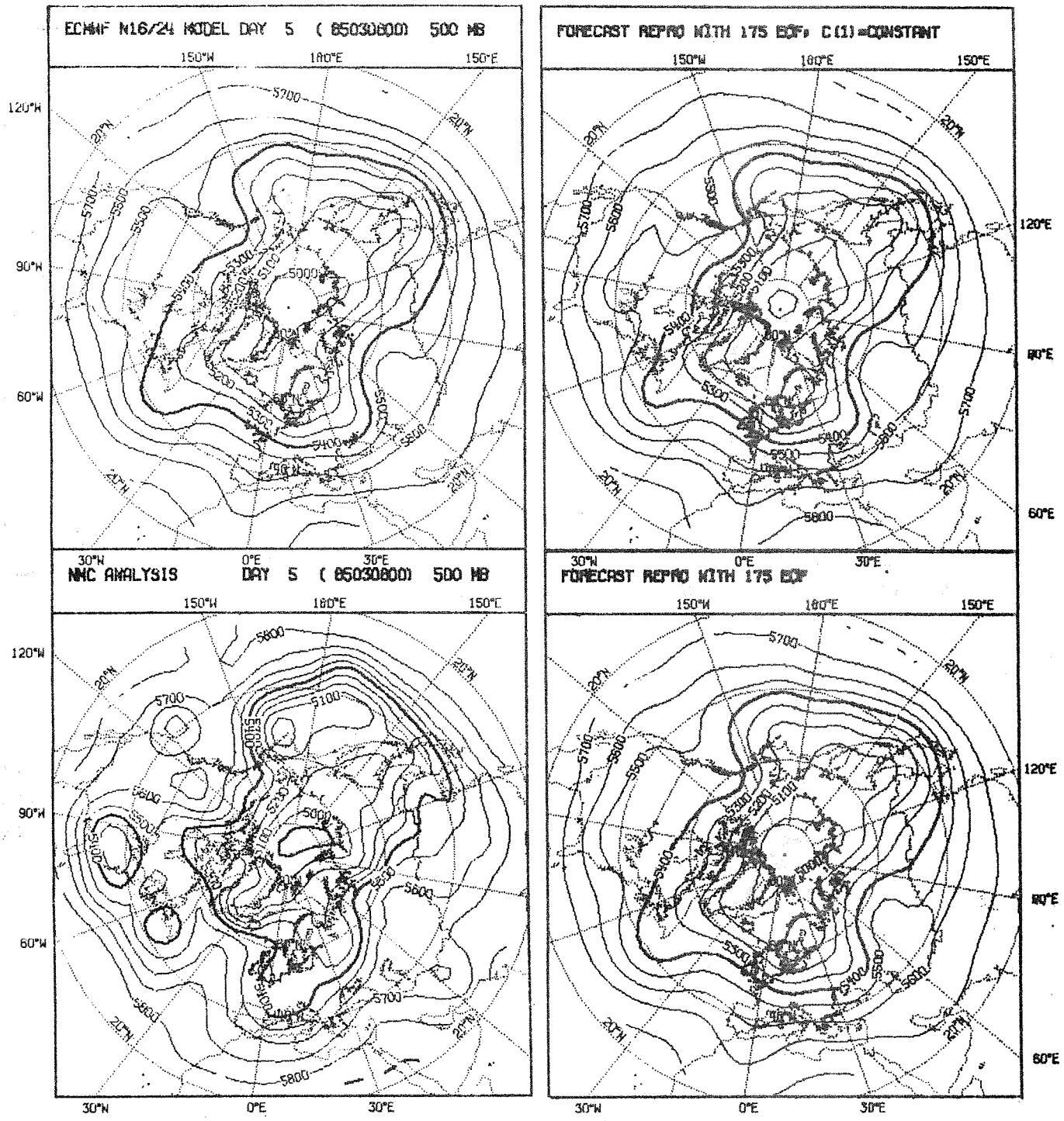

Fig. 11. Example of reproduced 500 mb height forecast for day 5 (8.3.1965 OGMT). In top right map the first e.o.f. coefficient is kept constant and equal to initial value.

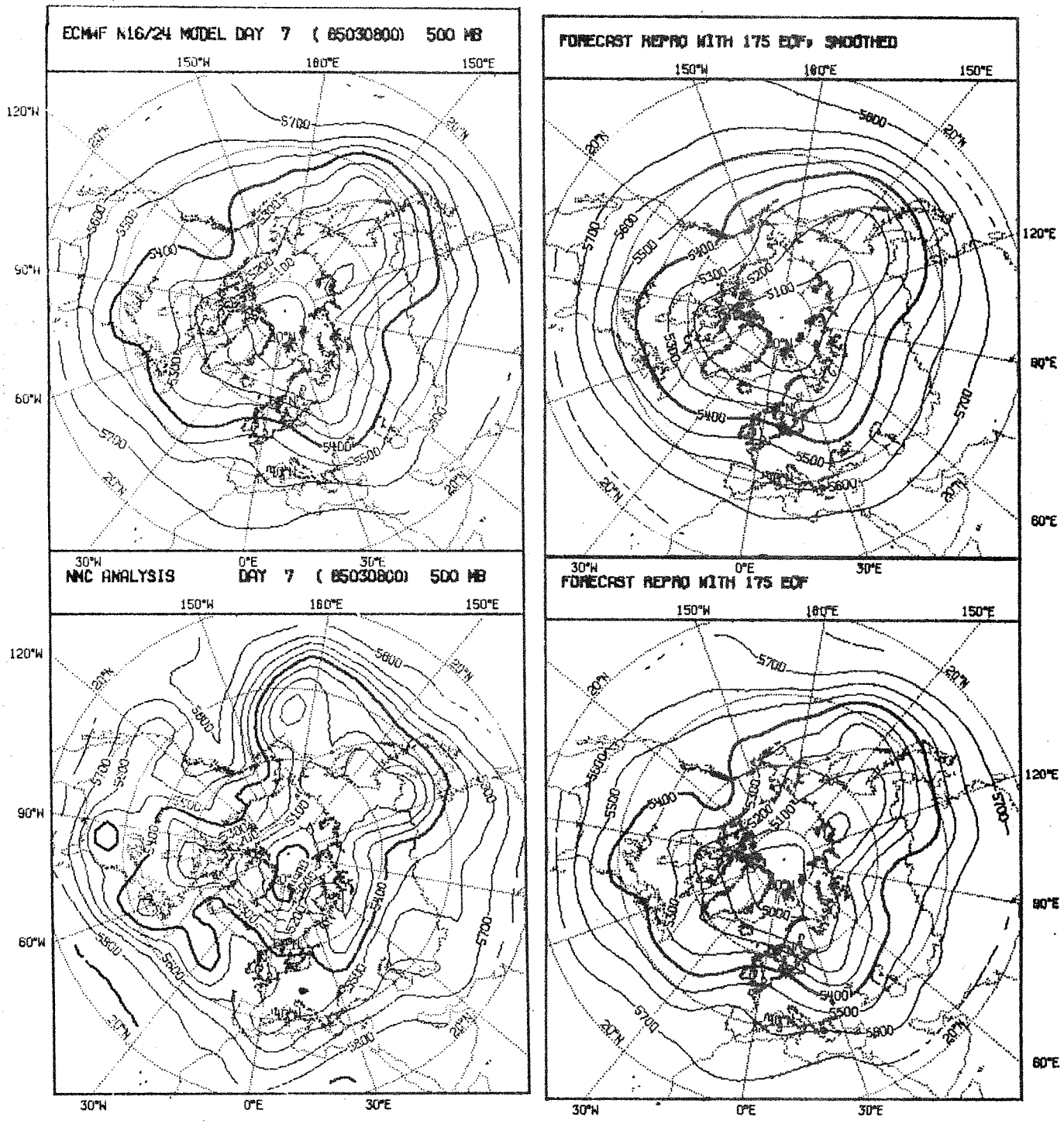

Fig. 12. As Fig. 11 but for day 7. In top right map the e.o.f. reproduction has been smoothed in addition to keeping c_1 constant.

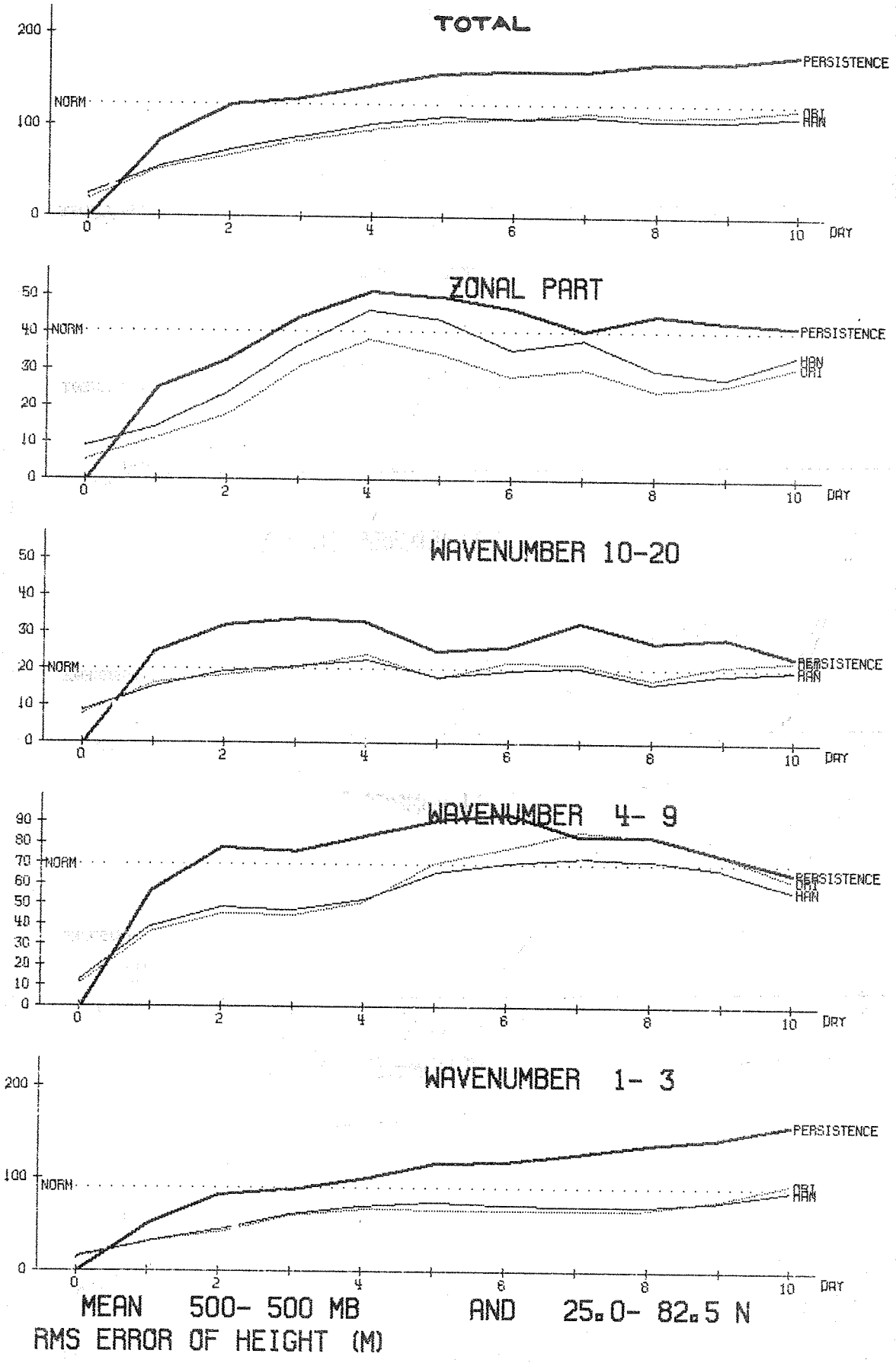

Fig. 13. 500 mb height rms error (m) in the original(ori) and smoothed (han) forecast.

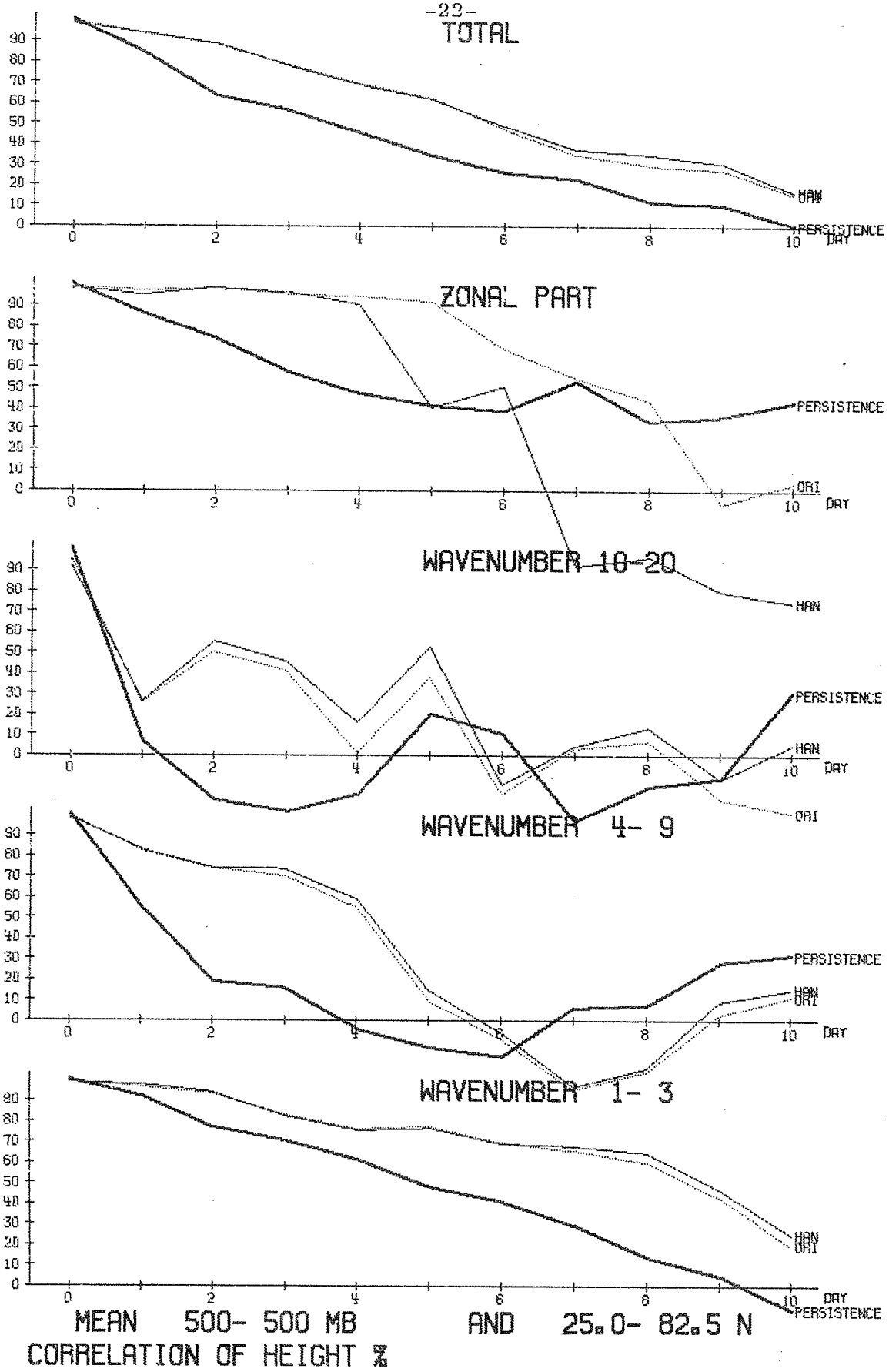

Fig. 14. 500 mb height anomaly correlation (%) in the original (ori) and smoothed (han) forecast.

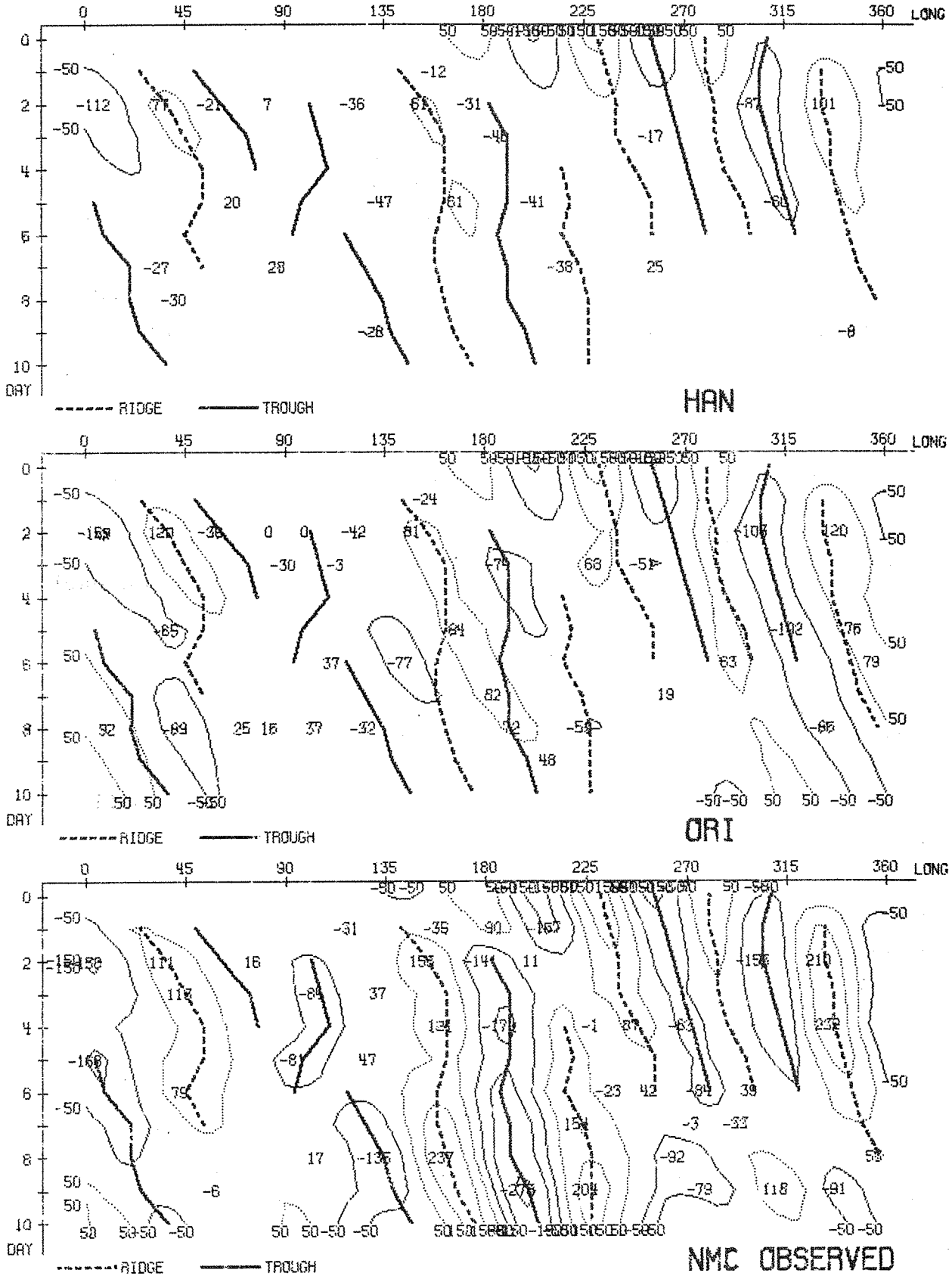

WAVENUMBER 4- 9 LATITUDE 45.0 N LEVEL 500 MB GEOP. HEIGHT

Fig.15. Hovmöller diagram of the original (ori) and smoothed (han) forecast and NMC analysis.

Although both the forecast model and the sample for e.o.f.'s used here are quite different, this type of smoothing was tried in addition to keeping c_1 constant. The rms error in Figure 10 for the 1404-grid point area is slightly smaller but only from day 6 onwards. Of course any smoothing should decrease rms error, but (5.2) seems to be optimal if all 175 degrees of freedom are used, according to a few test cases where parameters of B were varied. Figure 12 gives an example of the smoothed forecast for day 7.

To further evaluate this statistical correction the ECMWF conventional verification package was used, after interpolating the NMC grid values to 2.5° lat-long grid and calculating Fourier coefficients up to wave number 20 on each latitude line between 25° - 82.5° N (Arpe et al, 1976). After this procedure the total rms error of the original forecast is very near to the corrected and both are under normal variation line (Figure 13). The original forecast was better in zonal mean part both in rms error and correlation coefficient. However, in baroclinic and small wave number groups 4 - 9, 10 - 20, the smoothed forecast is slightly better after 4 days. The phases of the waves are practically unchanged,which is demonstrated by the Hovmöller ridge-trough diagram in Figure 15.

6. Comparison of e.o.f.'s and spherical harmonics in storing data.

One advantage of a series expansion is that normally less is needed to represent the field with reasonable accuracy than was the case with the original amount of information. The e.o.f. expansion is the most effective by definition in the sense of a least square fit in time and space, when applied to the data sample from where they were determined. An important question is how effective the e.o.f. expansion

is compared to a functional series, such as spherical harmonics, in independent data. To compare this storing effectivity a few northern hemisphere 500 mb height analyses were expanded into e.o.f. series (2.6) and into (surface) spherical harmonics series

$$z(\lambda,\phi) = \sum_{m=0}^{M} \sum_{n=m}^{N} (A_n^m \cos m\lambda + B_n^m \sin m\lambda) P_n^m(\sin\phi) \quad (6.1)$$

using the method of Machenhauer and Daley (1972). This method exploiting Gaussian quadrature was found slightly more accurate than the conventional method of trapezoidal integration over latitudes, which, furthermore, was unstable, if poles were grid points. Then truncation of the series (6.1) is usually either triangular (M=N=T) or rhomboidal (M=R, N=m+R), although the optimum truncation may be a combination of these.

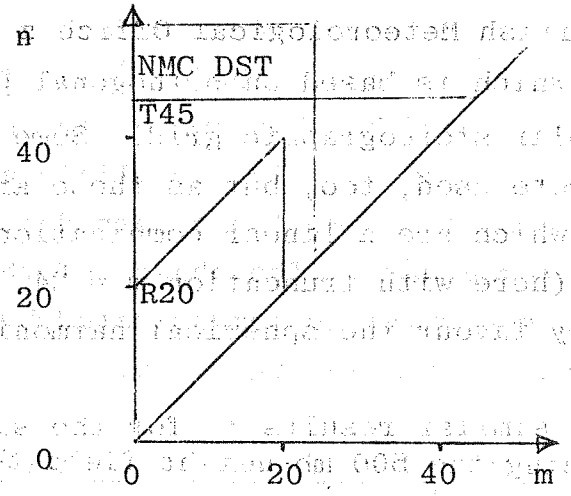

Fig. 16 . Examples of truncations used for the spherical harmonics expansion.

In the spherical harmonics expansion for northern hemisphere data only coefficients A_n^m, B_n^m with m+n = even ($B_n^0 = 0$) are used. The number of coefficients needed is then $(\frac{T}{2} + 1)$. (T + 1) for triangular truncation and $(\frac{R}{2} + 1)(2R + 1)$ for rhomboidal truncation (R even).

In Figure 17 the deviation measures between the truncated series reproductions and the original grid point field values are plotted as a function of numbers needed for storing in one case. The deviation measures are the maximum absolute deviation found in the area, rms deviation and that part of the surface, where deviation is more than a given tolerance, all for the area 22^oN - 90^oN.

The z 500 mb analysis used is taken from ECMWF's multivariate optimum interpolation scheme for 3.75^o lat-lon grid in 12.2 .76 12 z. The same deviation measures are in Figure 18 for the British Meteorological Office z 500 mb analysis in 8.2.76 0z, which is based on orthogonal polynomial fitting on 300 km polar stereographic grid. Some NMC DST 2.5^o grid analyses were used, too, but as these are based on Hough-functions, which are a linear combination of spherical harmonics (here with truncation m = 24, n = 55, Sela, 1974), they may favour the spherical harmonics expansion.
All these tests gave similar results : for the same accuracy in reproducing the 500 mb height field the spherical harmonics expansion needs about twice the amount of numbers, compared to e.o.f.'s. For example, the rms deviation to be less than 20 m in the BMO analysis 80 e.o.f. coefficients are needed but 153 (T16) for spherical harmonics series. It can also be seen that the triangular truncation is slightly better than rhomboidal in the storing sense.

E.o.f.'s thus seem to be twice as effective as spherical harmonics in data storing. However, the spherical harmonics

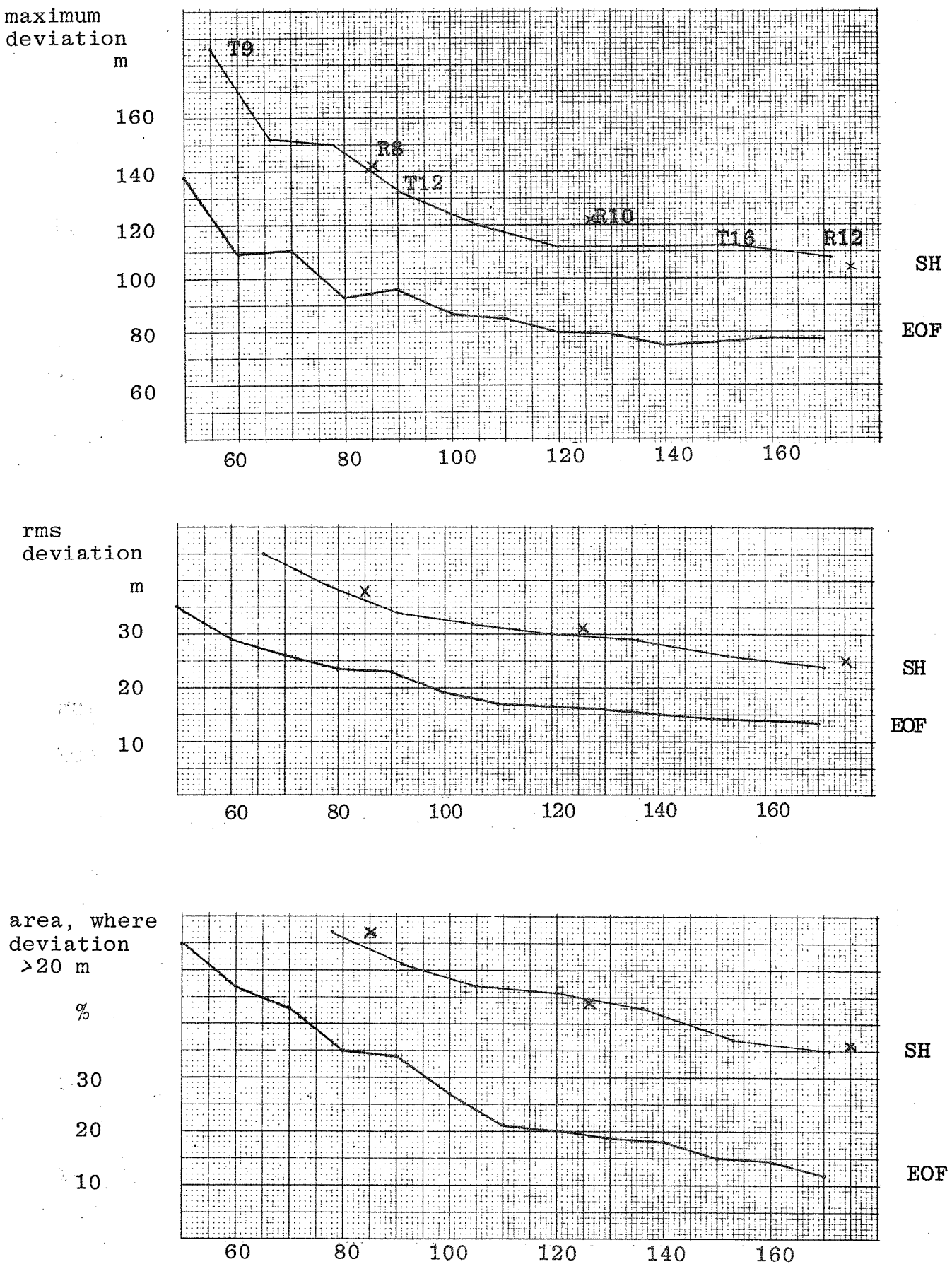

Fig. 17. Maximum deviation, rms deviation and area where deviation is greater than 20 m between original grid point field and the truncated series expansion as the function of the number of coefficients used. ECMWF 500 mb height analysis 12.2.1976 0Z, north of 22 ^{o}N. SH= spherical harmonics expansion
EOF= empirical orthogonal function expansion.

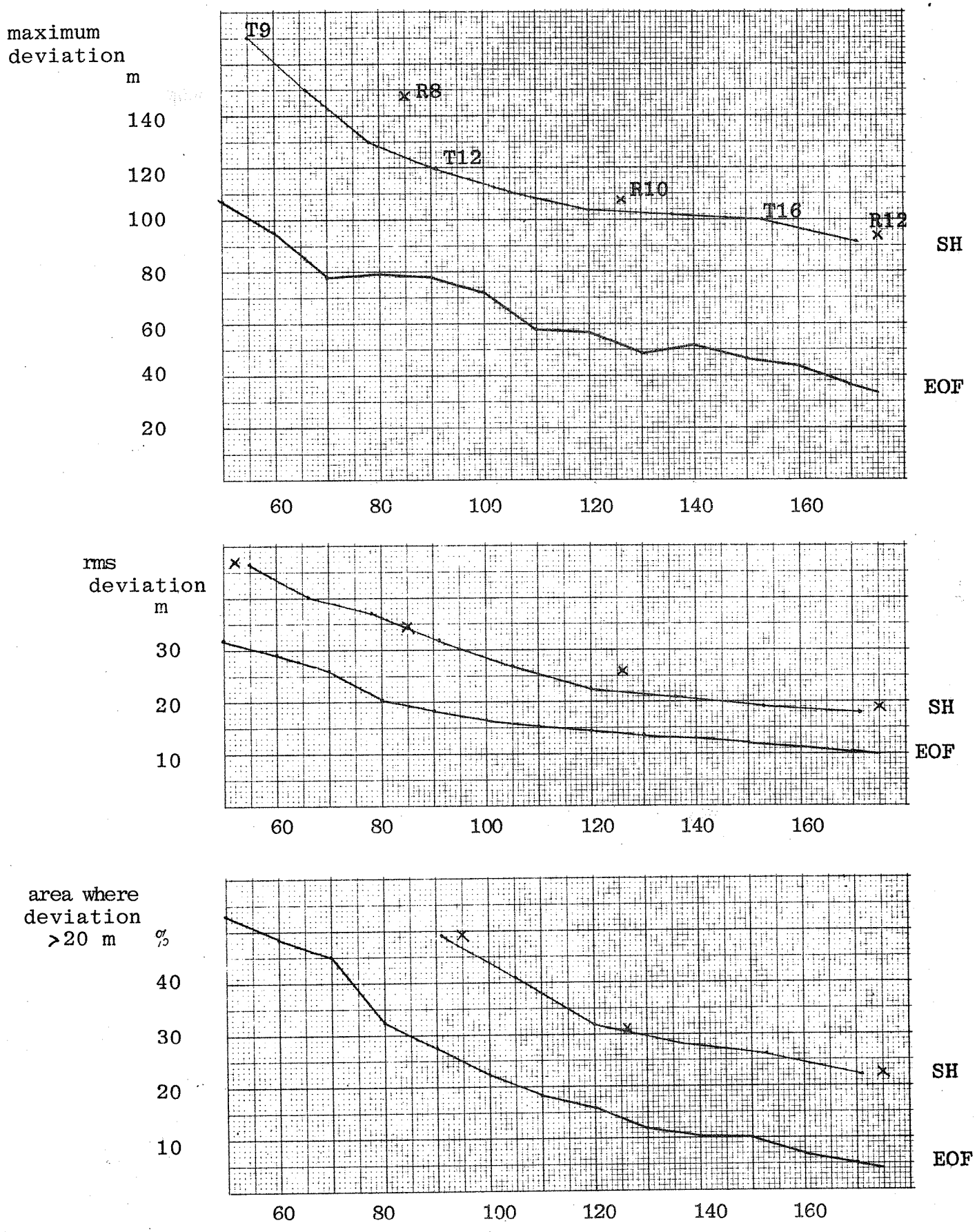

Fig. 18. Same as Fig. 17 but for British Meteorological Office, 8.2.1976 0Z
500 mb height analysis.

expansion is valid for the northern hemisphere, while the e.o.f. area was only north of 22°N. Furthermore, mathematical functions can be easily used in any level and for any variable while the determination of e.o.f.'s is always a rather laboursome task. Another question may arise about the time dependency of the e.o.f. series residual : an event which did not exist or was extremely rare in the original data sample cannot be represented by the series, and thus effectively filters out. This feature is not necessarily harmful, but it should be borne in mind when storing or filtering data with the aid of e.o.f.'s. A few tests were made, where the 500 mb height analysis was fed with Gaussian random noise with zero mean and standard deviation of 20 m, and/or small scale humps. All these cases gave coefficients (2.7) very near to the original coefficients, so that this random noise was effectively filtered out. On the other hand, if the artificial hump in a small area is considered a small scale low, it was filtered out as well. It is felt that extra studies are needed to evaluate these time dependent filtering properties.

The conclusion is that e.o.f. series is very useful for special purposes, e.g. high density storing for climatological studies, while general storing is more suitable to spherical harmonics or other functional representation because of their rather good effectiveness and more general nature.
Finally, to demonstrate the achievable accuracy with the spherical harmonics expansion Figure 19 gives the deviation scores up to T60 in DST (2.5° grid), BMO (300 km grid) and ECMWF (3.75° grid) analyses for the northern hemisphere. The smoothly varying 500 mb height field is well suited to a series expansion : deviations of all the three analyses converge towards zero quite rapidly. DST analysis is easiest to represent with spherical harmonics as can be expected.

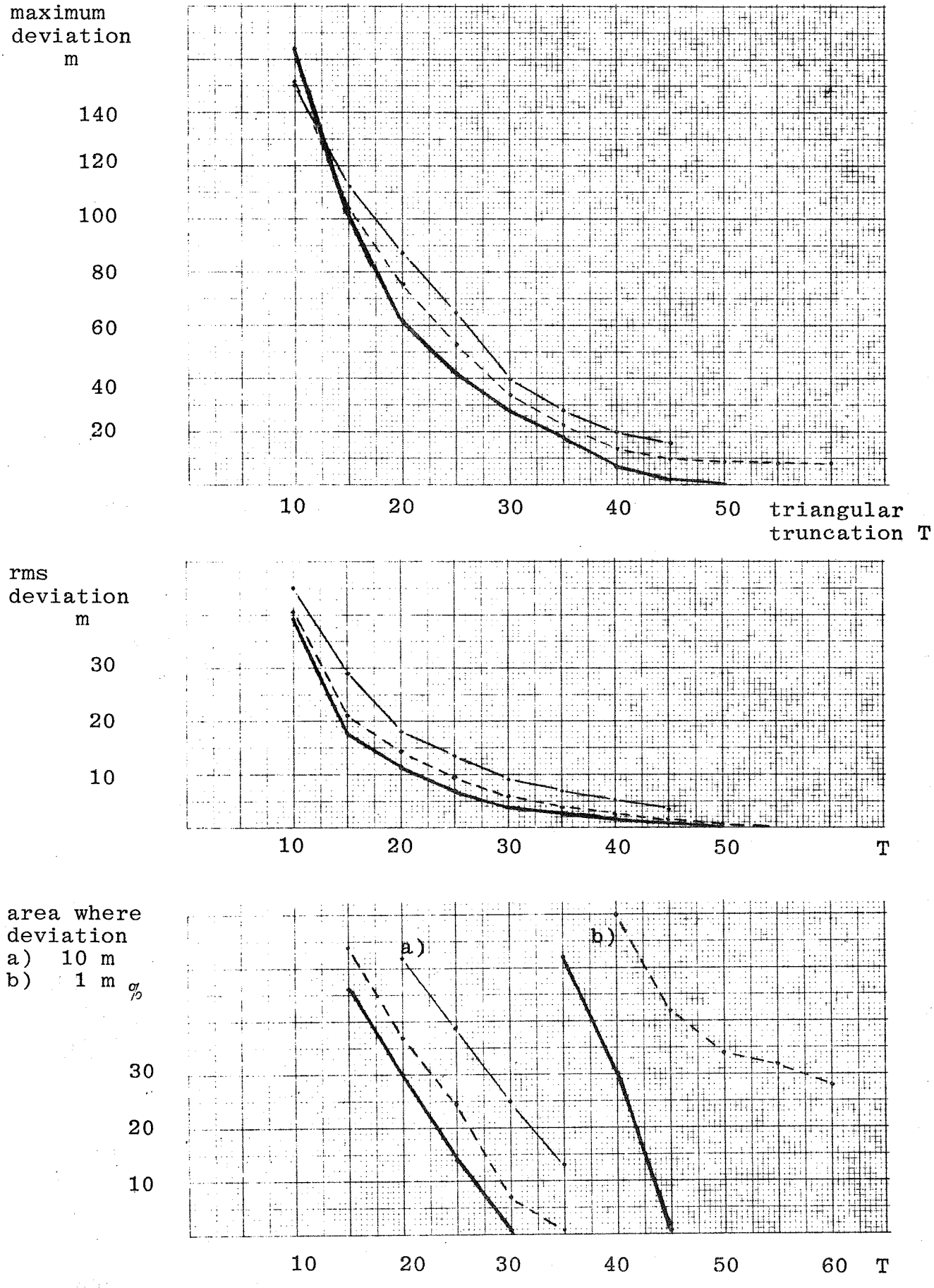

Fig. 19. Deviation between original grid point field and spherical harmonics expansion as the function of triangular truncation for 500 mb height analyses in northern hemisphere.

——— NMC DST 8.2.76 0Z 2.5° global grid
—— ECMWF 12.2.76 0Z 3.75° global grid
--- BMO 8.2.76 0Z 300 km polar stereographic grid

7. Conclusion

Empirical orthogonal functions (e.o.f.) for 500 mb height fields from a 20 years material have been used in studying different numerical analyses and an ECMWF 10 day forecast. The deviation between NMC, DWD and FNWC analyses was generally small with the largest deviation systematically in the second coefficient c_2. One third of the total rms deviation between the analyses (totally $\sim$ 30 m in the area north of 22^{o}N) was due to the first ten coefficients related to large scale phenomena. In the ten day forecast with the ECMWF model in N16/24, 9 level resolution and GFDL physics but Kuo convection, the largest error was in the first coefficient c_1, which is generally accepted to describe climatological features. Using persistence for this smoothly varying coefficient when reconstructing the forecast decreased the rms error about 10 %.
An optimized smoothing scheme for the coefficients was tested, but this did not have a great effect on error scores, and the smoothing tends to be strong for medium-range forecasts. Calculations on other cases to be published later confirm these results.

Comparing e.o.f.'s and spherical harmonics expansion (in triangular and rhomboidal truncation) using the same data gave the result that e.o.f.'s are about twice as effective in describing 500 mb height fields, when measured by grid point maximum deviation and rms deviation. However, the e.o.f.'s are less general and also act as a time filter, which may introduce problems in data storing and filtering. Their main use may thus be in the verification and diagnostics, Interesting problems in this area might be to find the time filtering properties, to develop new skill scores, which could be nearer to subjective evaluations than the present statistical scores, and to compare vertical e.o.f.'s from model forecasts with reality.

References:

Arpe, K., Bengtsson, L., Hollingsworth, A. and Janjić, Z.	1976	A case study of a ten day prediction. ECMWF Technical Report No. 1.
Craddock, J.F. and Flood, C.R.	1969	Eigenvectors for representing the 500 mb geopotential surface over the Northern Hemisphere. Q.J.R.M.S. 95, 576 - 593.
ECMWF	1977	Workshop on the use of e.o.f. in Meteorology. ECMWF Proceedings.
Haltiner, G.J.	1971	Numerical Weather Prediction. Wiley & Sons, 317 pp.
Holmström, I.	1977	On empirical orthogonal functions and variational methods. Workshop on the use of e.o.f. in Meteorology. ECMWF, 21 - 26 .
van Loon, H. and Rogers, J.C.	1978	The seesaw in winter temperatures between Greenland and Northern Europe. Part I. Mon. Wea. Rev. 106, 296 - 310.
Karhila, V. and Rinne, J.	1977	Determination of empirical orthogonal functions from a large sample. Workshop on the use of e.o.f, in Meteorology. ECMWF, 84 - 96.

References:

Machenhauer, B. and Daley, R.	1972	A baroclinic primitive equation model with a spectral representation in three dimensions. Institut for teoretisk meteorologi, København Universitet Report No.4
Otto-Bliesner, B. Baumhefner, D.P., Schlatter, T.W. and Bleck, R.	1977	A comparison of several meteorological analysis schemes over a data-rich region. Mon. Wea. Rev. 105, 1083 - 1091.
Rinne, J.	1972	Investigation of the forecasting error of a simple barotropic model with the aid of empirical orthogonal functions. Part III. Geophysica 12/1, 57 - 78.
Rinne, J.	1977	Controlling a large data sample with the aid of empirical orthogonal functions. Workshop on the use of e.o.f. in Meteorology. ECMWF, 134 - 140.
Rinne, J. and Järvenoja,S.	1977	Accuracy of the series given in empirical orthogonal functions. Workshop on the use of e.o.f. in Meteorology. ECMWF, 97 - 112.
Rinne, J. and Karhila, V.	1975	A spectral barotropic model in horizontal empirical orthogonal functions. Q.J.R.M.S. 101, 365-382.
Sela, J.	1974	Hough functions to spherical harmonics data transformation. GARP Report No. 7, 131 - 138.

References :

Tiedtke, M. 1977 The parameterization scheme of the ECMWF grid point model. ECMWF Seminars, 1977.

EUROPEAN CENTRE FOR MEDIUM RANGE WEATHER FORECASTS

Research Department (RD)

Internal Report No. 18

No. 1 Users Guide for the GFDL Model (November 1976)

No. 2 The effect of Replacing Southern Hemispheric Analyses by Climatology on Medium Range Weather Forecasts (January 1977)

No. 3 Test of a Lateral Boundary Relaxation Scheme in a Barotropic Model (February 1977)

No. 4 Parameterization of the Surface Fluxes (February 1977)

No. 5 An Improved Algorithm for the Direct Solution of Poisson's Equation over Irregular Regions (February 1977)

No. 6 Comparative Extended Range Numerical Integrations with the ECMWF Global Forecasting Model 1 : The N24, Non-Adiabatic Experiment (March 1977)

No. 7 The ECMWF Limited Area Model (March 1977)

No. 8 A Comprehensive Radiation Scheme designed for Fast Computation (May 1977)

No. 9 Documentation for the ECMWF Grid-Point Model (May 1977)

No. 10 Numerical Tests of Parameterization Schemes at an Actual Case of Transformation of Arctic Air (June 1977)

No. 11 Analysis Error Calculations for the FGGE (June 1977)

No. 12 Normal Modes of a Barotropic Version of the ECMWF Grid-Point Model (July 1977)

No. 13 Direct Methods for the Solution of the Discrete Poisson Equation : Some Comparisons (July 1977)

No. 14 On the FACR (ℓ) Algorithm for the Discrete Poisson Equation (September 1977)

No. 15 A Routine for Normal Mode Initialization with Non-Linear Correction for a Multi-Level Spectral Model with Triangular Truncation (August 1977)

No. 16 A Channel Version of the ECMWF Grid-Point Model (December 1977)

No. 17 A Comparative Study of Some Low Resolution Explicit and Semi-Implicit Spectral Integrations (August 1978)

EUROPEAN CENTRE FOR MEDIUM RANGE WEATHER FORECASTS

Research Department (RD)

Internal Report No. 18

No. 18 Verification and Storing with Empirical Orthogonal Functions (printed in November 1978)

No. 19 Documentation of the ECMWF Spectral Model (October 1978)